JCTC Journal of Chemical Theory and Computation

pubs.acs.org/JCTC

Article

Quantum Nature of Ubiquitous Vibrational Features Revealed for Ethylene Glycol

Apurba Nandi,* Riccardo Conte,* Priyanka Pandey, Paul L. Houston, Chen Qu, Qi Yu, and Joel M. Bowman*

Cite This: J. Chem. Theory Comput. 2025, 21, 5208−5220

Read Online

ACCESS | Metrics & More | Article Recommendations | Supporting Information

ABSTRACT: Vibrational properties of molecules are of widespread interest and importance in chemistry and biochemistry. The reliability of widely employed approximate computational methods is questioned here against the complex experimental spectrum of ethylene glycol. Comparisons between quantum vibrational self-consistent field and virtual-state configuration interaction (VSCF/VCI), adiabatically switched semiclassical initial value representation (AS-SCIVR), and thermostatted ring polymer molecular dynamics (TRPMD) calculations are made using a full-dimensional, machine-learned potential energy surface. Calculations are done for five low-lying conformers and compared with the experiment, with a focus on the high-frequency, OH-stretches, and CH-stretches, part of the spectrum. Fermi resonances are found in the analysis of VSCF/VCI eigenstates belonging to the CH-stretching band. Results of comparable accuracy, quality, and level of detail are obtained by means of AS SCIVR. The current VSCF/VCI and AS-SCIVR power spectra largely close the gaps between the experiment and TRPMD and classical MD calculations. Analysis of these results provides guidance on what level of accuracy to expect from TRPMD and classical MD calculations of the vibrational spectra for ubiquitous CH- and OH-stretching bands. This work shows that even general vibrational features require a proper quantum treatment, usually not achievable by the most popular theoretical approaches.

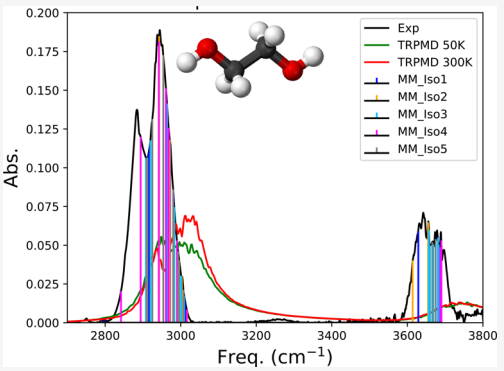

INTRODUCTION

The importance of intramolecular hydrogen bonding on the conformation of biomolecules is well-established. Ethylene glycol, depicted in Figure 1, attracted the attention of experimentalists as being a small molecule where this intramolecular hydrogen bonding might occur, due to the two hydroxyl groups. This was investigated in the recent paper by Das et al.[1] That paper focused on the signature of this bonding in the IR spectrum under conditions of low concentration in the gas phase at 303, 313, and 323 K and concluded that, such bonding is not present. In addition, an analysis of the thermal contribution of ten low-lying conformers to the IR spectrum was made using the double-harmonic approximation based on DFT calculations (B3LYP/aug-cc-pVDZ).

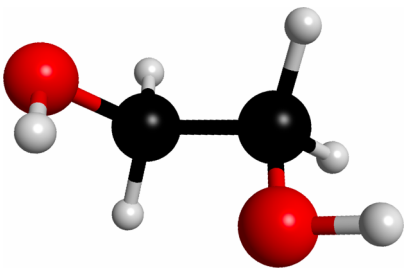

Figure 1. Global minimum structure of ethylene glycol.

This molecule has also been studied by several theoretical chemists with great interest due to controversy on the existence of intramolecular hydrogen bonding and its complex torsional landscape via three torsional degrees of freedom (the OCCO and two HOCC dihedrals).

Recently, Arandhara and Ramesh reported an interesting study of quantum effects in the temperature-dependent structure of ethylene glycol. They used path integral and classical molecular dynamics as well as classical and thermostatted ring-polymer molecular dynamics (TRPMD)[2] of the vibrational power spectrum of ethylene glycol, using a new full-dimensional potential energy surface (PES).[3] The PES was a fit to 18,772 MP2/aug-cc-pVTZ energies concentrated in the region of a reduced dimensionality space determined by

Received: January 30, 2025
Revised: April 18, 2025
Accepted: April 21, 2025
Published: May 7, 2025

minimizing the energy with respect to three dihedral angles. The full PES is given by the sum $V_{rs} + V_b$, where V_{rs} is the three-degree-freedom minimized potential referred as 'reaction surface' potential and V_b is a power-fit to energies displaced from the minimized surface. We omit the details of this elaborate representation and refer the interested reader to their paper and Supporting Information for details.[3] We do use this PES for limited calculations, as described below.

The classical and TRPMD vibrational power spectra reported using this PES are of particular interest to us, as these relate to experimental IR spectra and also motivate the work we present here. These power spectra were compared to experiment for the OH and CH-stretch bands at 300 K, where several conformers contribute significantly to these spectra. In both the classical and TRPMD approaches the power spectrum is obtained from the Fourier transform of the velocity autocorrelation function, either at fixed total energy in the case of microcanonical classical MD or fixed temperature in the case of TRPMD.[2] TRPMD uses ring-polymer molecular dynamics[4] coupled to a thermostat[5] as a means to obtain quantum thermal effects, mainly zero-point energy (ZPE) effects. There is no explicit quantization of excited vibrational motion in TRPMD, and if a single bead is used then TRPMD becomes canonical classical MD. An incisive and insightful review of these methods can be found in ref 6.

As we review below, both calculated spectra are upshifted from the experiment, with the classical one more so than the TRPMD one. Of course, this may be due to errors inherent in both approaches or the PES or both. Evidence for the former was recently presented by Qi and Bowman for $H_7O_3^+$ and $H_9O_4^+$.[7] In that work the IR spectrum was calculated using these methods and vibrational self-consistent field/virtual-state configuration interaction (VSCF/VCI)[8−10] calculations, all using accurate potential and dipole moment surfaces. Excellent agreement with the experiment was seen with the VSCF/VCI calculations. These closed a large gap between the experiment and classical and also the smaller gap with TRPMD, both with respect to band positions and widths.

Here we report a new fit to these electronic energies and gradients using our permutationally invariant polynomial (PIP) approach.[11,12] The new PES is used in VSCF/VCI and adiabatically switched semiclassical initial value representation (AS-SCIVR)[13,14] calculations of the power spectrum. Calculations are done for five low-lying conformers and compared with the experiment, with a focus on the high-frequency, OH, and CH-stretches. Fermi resonances are found in the analysis of VSCF/VCI eigenstates belonging to the CH-stretching band. Results of comparable accuracy, quality, and level of detail are obtained by means of AS SCIVR. Comparisons are also made with classical and TRPMD calculations of the vibrational power spectrum by Mrinal and Ramesh, using their fit to these electronic energies. The current VSCF/VCI and AS-SCIVR power spectra largely close the gap between the experiment and these previous classical and TRPMD calculations. Discussion of these comparisons sheds additional light on the limitations of these methods.

The paper is organized as follows. A brief review of the theoretical methods is given followed by computational details. Following that results and discussion are given, and we conclude with a summary and conclusions.

THEORY AND COMPUTATIONAL DETAILS

Linear Regression with Permutationally Invariant Polynomials. Here we employ the well-established permutationally invariant polynomial (PIP) approach[11,15,16] to fit the full-dimensional PES of ethylene glycol. The theory of this PIP approach has been presented in several review articles[11,12,17−19] and therefore we are not presenting it in great detail. In terms of a PIP basis, the potential energy, V, can be written in compact form as

$$V(\boldsymbol{x}) = \sum_{i=1}^{n_p} c_i p_i(\boldsymbol{x}) \tag{1}$$

where c_i are linear coefficients, p_i are PIPs, n_p is the total number of polynomials for a given maximum polynomial order, and $\boldsymbol{x}$ are Morse variables. For example, $x_{\alpha\beta}$ is given by $\exp(-r_{\alpha\beta}/\lambda)$, where $r_{\alpha\beta}$ is the internuclear distance between atoms α and β. The range (hyper)parameter, λ, was chosen as 2 bohr.

Optimal parameters such as the coefficients (c) are obtained by minimizing the loss function.

$$L(c) := \sum_X (w_X^E |E(c;X) - E_{QM}(X)|^2 + w_X^F |F(c;X) - F_{QM}(X)|^2) \tag{2}$$

Where E_{QM} and F_{QM} are the energies and corresponding forces in the training data set, obtained from direct electronic structure calculations. The sum is taken over all configurations in the training data set, and w_X^E and w_X^F are the weights specifying the relative importance of energies and forces. Here we use equal weights for both energy and forces ($w_X^E = w_X^F = 1$). As energy and force are both linear in the free parameters, the loss can be written in a linear least-squares form

$$L(c) := \|\xi c - t\|^2 \tag{3}$$

where the vector t contains the direct QM energy and force observations and the design matrix ξ contains the values of the PIP basis and the negative gradients of the PIP basis evaluated at the training geometries. The number of rows of ξ equal to the total number of observations (energies and force components) in the training data set and the number of columns equal to the total number of basis functions. More often this linear regression problem can be regularized by modifying the loss function as

$$L(c) := \|\xi c - t\|^2 + \eta \|\Gamma c\|^2 \tag{4}$$

where Γ is the identity matrix. However, we did not regularize the loss $L(c)$ function as the number of rows of the ξ matrix is much larger than the number of unknown coefficients c.

In order to develop the PES a total of 18,772 MP2/aug-cc-pVTZ energies and the corresponding forces (a total data size of 581,932) are employed. This data set was generated by Arandhara and Ramesh and we have taken from their recently reported article.[3] A maximum polynomial order of 4 with permutational symmetry of 22222 is employed. Referring to Figure 1, this notation indicates that the 2 O atoms are treated as identical as well as the two H atom in the two OH groups. In short-hand notation this is "22". Then the C atoms are treated as identical as are the 2 H atoms in each CH2 group, so that is indicated finally by "22222". This results in a total of 16,981 PIPs and thus linear coefficients. These PIP bases are generated using MSA software.[15,20] The optimized coefficients

https://doi.org/10.1021/acs.jctc.5c00173
J. Chem. Theory Comput. 2025, 21, 5208−5220

are obtained by solving the above least-squares linear algebra (eq 4) with the freely available FORTRAN code DGELSS.

MULTIMODE Calculations. Post-harmonic quantum methods based on vibrational self-consistent field (VSCF) and virtual-state configuration interaction (VCI) approaches have been known for almost 50 years. These methods have been implemented in our software called MULTIMODE. First, we present a brief recap of the VSCF[8,9] and VSCF/VCI scheme[10] in MULTIMODE.[21−23] The computational code is based on the rigorous Watson Hamiltonian[24] in mass-scaled normal coordinates, $\mathbf{Q}$, for nonlinear molecules. This Hamiltonian is given by

$$\hat{H} = \frac{1}{2}\sum_{\alpha\beta}(\hat{J}_\alpha - \hat{\pi}_\alpha)\mu_{\alpha\beta}(\hat{J}_\beta - \hat{\pi}_\beta) - \frac{1}{2}\sum_{k}^{F}\frac{\partial^2}{\partial Q_k^2} - \frac{1}{8}\sum_{\alpha}\mu_{\alpha\alpha} + V(\mathbf{Q}) \tag{5}$$

where $\alpha(\beta)$ represent the x, y, z coordinates, $\hat{J}_\alpha$ and $\hat{\pi}_\alpha$ are the components of the total and vibrational angular momenta respectively, $\mu_{\alpha\beta}$ is the inverse of effective moment of inertia tensor, and $V(\mathbf{Q})$ is the full potential in terms of normal coordinates. The number of normal modes is denoted by F, and for nonlinear molecules F equals $3N - 6$. In many applications of this Hamiltonian in the literature, the vibrational angular momentum terms are neglected without justification. We examine this below, where we present results, as we always do including this term, and where we neglect it. Therefore, we include these terms in the MULTIMODE software.

In general, there are two major bottlenecks in applications to the VSCF/VCI scheme. One is the numerical evaluation of matrix elements (multidimensional integrals) and the second is the size of the H-matrix. Both naively have exponential dependence on the number of normal coordinates. An effective approach to deal with exponential scaling of matrix elements we represent the full potential in a hierarchical n-mode representation (nMR).[21] In normal coordinates, this representation is given by

$$\begin{aligned} V(Q_1, Q_2, \cdots, Q_F) &= \sum_i V_i^{(1)}(Q_i) + \sum_{i,j} V_{ij}^{(2)}(Q_i, Q_j) \\ &+ \sum_{i,j,k} V_{ijk}^{(3)}(Q_i, Q_j, Q_k) + \sum_{i,j,k,l} V_{ijkl}^{(4)}(Q_i, Q_j, Q_k, Q_l) \\ &+ \cdots \end{aligned} \tag{6}$$

where $V_i^{(1)}(Q_i)$ is the one-mode potential, i.e., the 1D cut through the full-dimensional PES in each mode, one-by-one, $V_{ij}^{(2)}(Q_i, Q_j)$ is the intrinsic 2-mode potential among all pairs of modes, etc. Here, intrinsic means that any n-mode term is zero if any of the arguments is zero. Also, each term in the representation is in principle of infinite order in the sense of a Taylor series expansion. So for example, $V^{(1)}(Q)$ might look like a full Morse potential.

This representation has been used for nearly 20 years by a number of research groups; a sample of these are refs 21−23 and 25−28. It continues to be actively used in a variety of applications and theoretical developments.[29−34] In MULTIMODE the maximum value of n is 6. However, from numerous tests it appears that a 4MR typically gives energies that are converged to within roughly 1−5 cm^{-1}.[35−37] Thus, we generally use 4MR with an existing full-dimensional PES and this is also done here.

The second major bottleneck to all VCI calculations is the diagonalization of the H-matrix, which as noted already can scale exponentially with the number of vibrational modes. This matrix results in the usual way following the VCI expansion of wave functions given in simplified notation by

$$\Psi_L = \sum_K c_K^{(L)}\Phi_K \tag{7}$$

where Φ_K are a complete, orthonormal set of functions. In the VSCF/VCI approach, these are the eigenfunctions of the VSCF Hamiltonian operator for the ground vibrational state. There are many strategies to deal with this. Basically, they all limit the size of the excitation space, with many schemes taken from electronic structure theory. For example, the excitation space can be limited by using the hierarchical scheme of single, double, triple, etc. excitations. MULTIMODE uses this among other schemes and can consider up to quintuple excitations. A major difference with electronic structure theory is that the nuclear interactions go beyond 2-body. This is immediately clear from the n-mode representation. Thus, MULTIMODE tailors the excitation scheme for each term in this representation. Other schemes to prune the CI basis have been suggested and the reader is referred to reviews[27,29,35,38−43] for more details and specific details for the present calculations are given in the Supporting Information (SI). We note that in the present case, an iterative diagonalization routine is used to obtain the eigenvalues and eigenvectors of the H-matrix. The eigenvalues are VSCF/VCI quantum vibrational energies, E_L with corresponding eigenvectors, i.e., the expansion coefficients, $c_K^{(L)}$.

In this paper, where the vibrational IR and power spectra play a central role, we make the following important remarks. First, the quantum power spectrum is rigorously just the distribution of *all* vibrational eigenvalues vs the energy. This can simply be visualized as vertical sticks of say unit height at the energies E_L. This spectrum of energies is not the IR spectrum. Indeed, this theoretical spectrum is virtually impossible to measure using IR and even IR and Raman spectroscopy. The reason comes from well-known selection and propensity rules governing these spectroscopies. In the present case, where low-resolution experimental IR spectra are compared with calculations the textbook selection "Δv" = 1 condition for IR intensities is assumed to hold. Of course, the IR spectrum can be calculated rigorously if the coordinate-dependent molecular dipole surface is available. Unfortunately, that surface is not available. The second remark is how we calculate a quantum power spectrum that can be reasonably compared to the IR spectrum and to the other calculated power spectra (more comments about these are given below). The approach we take is to examine the expansion coefficients for all the quantum states obtained with the vibrational bands of interest here, namely the OH- and the CH-stretch bands. We filter out just those states with dominant expansion coefficient(s) for one quantum of excitation in the OH-stretch or the CH-stretch for a given conformer i, $C_{(CH/OH)}^{Conf\{i\}}$, apply Gaussian broadening and thermal weighting. Thus, the working formula to estimate intensity is

$$I(E_{CH/OH}^{Conf\{i\}}) \propto wt^{Conf\{i\}} \cdot |C_{(CH/OH)}^{Conf\{i\}}|^2;\ \forall\ \{i\} \rightarrow 1, 2, \ldots, 5 \tag{8}$$

https://doi.org/10.1021/acs.jctc.5c00173
J. Chem. Theory Comput. 2025, 21, 5208−5220

$$I(E_{\mathrm{CH/OH}}^{\mathrm{Conf}\{i\}}) \approx I(\mathrm{constant})\cdot \mathrm{wt}^{\mathrm{Conf}\{i\}}\cdot |C_{(\mathrm{CH/OH})}^{\mathrm{Conf}\{i\}}|^2 \quad (9)$$

where $I(\mathrm{constant})$ is the arbitrary constant value, $\mathrm{wt}^{\mathrm{Conf}\{i\}}$ is the corresponding Boltzmann weight. This eq 9 is followed to estimate the intensity of CH- or OH-stretches for each conformer from MULTIMODE calculations.

AS-SCIVR Calculations. The adiabatically switched semiclassical initial value representation (AS-SCIVR) is a recently developed two-step semiclassical approach[13,14] able to regain quantum effects starting from classical trajectories. It differs from standard semiclassical techniques[44,45] in the way the starting conditions of the semiclassical dynamics run are selected. In AS-SCIVR a preliminary adiabatic switching[46] dynamics is performed, a procedure not present in previous semiclassical techniques. This allows one to start from an approximate true quantization of the initial conditions. Therefore, the exit atomic positions and momenta of the adiabatic switching run serve as starting conditions for the subsequent semiclassical dynamics trajectory.

The adiabatic switching Hamiltonian is[47−49]

$$H_{\mathrm{as}} = [1 - \lambda(t)]H_{\mathrm{harm}} + \lambda(t)H_{\mathrm{anh}} \quad (10)$$

where $\lambda(t)$ is the following switching function

$$\lambda(t) = \frac{t}{T_{\mathrm{AS}}} - \frac{1}{2\pi}\sin\left(\frac{2\pi t}{T_{\mathrm{AS}}}\right) \quad (11)$$

H_{harm} is the harmonic Hamiltonian built from the harmonic frequencies of vibration, and H_{anh} is the actual molecular vibrational Hamiltonian. In our simulations T_{AS} has been chosen equal to 25,000 a.u. (about 0.6 ps) and time steps of 10 a.u. have been employed. 4000 trajectories were evolved in each AS-SCIVR calculation. The AS-SCIVR zero-point energy estimate has been obtained by starting the AS run with no quanta of excitation in the modes, i.e. from the harmonic zero-point energy. Conversely, AS-SCIVR estimates of CH- and OH-stretches have been obtained by starting the AS run with an additional quantum of harmonic excitation to the specific mode under investigation. AS-SCIVR calculations have been performed for the global minimum geometry.

Once the adiabatic switching run is over, the trajectories are evolved according to H_{anh} for another 25,000 a.u. with the same step size to collect the dynamical data needed for the semiclassical calculation. This relies on Kaledin and Miller's time-averaged version of semiclassical spectroscopy. Therefore, the working formula is

$$I_{\mathrm{as}}(E) = \left(\frac{1}{2\pi\hbar}\right)^F \sum_{j=1}^{N_{\mathrm{traj}}} \frac{1}{2\pi\hbar T}\left| \int_0^T dt e^{i/\hbar[S_t^{(j)}(\mathbf{p}_{\mathrm{as}},\mathbf{q}_{\mathrm{as}}) + Et + \phi_t^{(j)}(\mathbf{p}_{\mathrm{as}},\mathbf{q}_{\mathrm{as}})]} \langle \Psi(\mathbf{p}_{\mathrm{eq}}, \mathbf{q}_{\mathrm{eq}}) | g^{(j)}(\mathbf{p}_t', \mathbf{q}_t')\rangle \right|^2 \quad (12)$$

where $I_{\mathrm{as}}(E)$ indicates that a vibrational spectral density is calculated as a function of the vibrational energy E. In eq 12, $F = 24$ in the case of ethylene glycol. T is the total evolution time of the dynamics for the semiclassical part of the simulation. As anticipated, we chose T equal to 25,000 a.u. with a time step size of 10 a.u. $(\mathbf{p}_t', \mathbf{q}_t')$ is the instantaneous full-dimensional phase-space trajectory started at time 0 from the final phase space condition $(\mathbf{p}_{\mathrm{as}}, \mathbf{q}_{\mathrm{as}})$ of the adiabatic switching part of the simulation. S_t is the classical action along the semiclassical trajectory, and ϕ_t is the phase of the Herman-Kluk pre-exponential factor based on the elements of the stability matrix and defined as

$$\phi_t = \mathrm{phase}\left[\sqrt{\left|\frac{1}{2}\left(\frac{\partial \mathbf{q}_t'}{\partial \mathbf{q}_{\mathrm{as}}} + \Gamma^{-1}\frac{\partial \mathbf{p}_t'}{\partial \mathbf{p}_{\mathrm{as}}}\Gamma - i\hbar\frac{\partial \mathbf{q}_t'}{\partial \mathbf{p}_{\mathrm{as}}}\Gamma + \frac{i\Gamma^{-1}}{\hbar}\frac{\partial \mathbf{p}_t'}{\partial \mathbf{q}_{\mathrm{as}}}\right)\right|}\right] \quad (13)$$

where Γ is an $N_v \times N_v$ matrix usually chosen to be diagonal with elements numerically equal to the harmonic frequencies.

Classical chaotic dynamics can lead to numerical inaccuracies in the semiclassical propagation, so, following a common procedure in semiclassical calculations, we have rejected the trajectories based on a 1% tolerance threshold on the monodromy matrix determinant value (which should be equal to 1 along the entire trajectory).[50] In the case of ethylene glycol this led to a rejection rate between 75 and 80% of trajectories. Finally, the working formula is completed by a quantum mechanical overlap between a quantum reference state $|\Psi\rangle$ and a coherent state $|g\rangle$ characterized by the following representation in configuration space

$$\langle \mathbf{q}|g(\mathbf{p}_t', \mathbf{q}_t')\rangle = \left(\frac{\det(\Gamma)}{\pi^F}\right)\exp\left\{-(\mathbf{q} - \mathbf{q}_t')^T\frac{\Gamma}{2}(\mathbf{q} - \mathbf{q}_t') + \frac{i}{\hbar}\mathbf{p}_t'^T(\mathbf{q} - \mathbf{q}_t')\right\} \quad (14)$$

The reference state $|\Psi\rangle$ is usually chosen to be itself a coherent state. In eq 12 $|\Psi\rangle$ is written as $|\Psi(\mathbf{p}_{\mathrm{eq}}, \mathbf{q}_{\mathrm{eq}})\rangle$, where $\mathbf{p}_{\mathrm{eq}}$ stands for the linear momenta obtained in harmonic approximation setting the geometry at the equilibrium one $(\mathbf{q}_{\mathrm{eq}})$.

Finally, we stress that this approach to the power spectrum is general and powerful, but it does not in practice resolve the quantum power spectrum discussed above in the way MULTIMODE does. This is due in large part to the finite time of the adiabatic switching, which results in a spread of the semiclassical energy.[46] The input for each band is a semiclassical approximation to a fundamental excitation in the OH- and CH-stretching modes. So the dominant signal is for these excitations. The method can in principle also resolve weak combination bands at higher energies built on the fundamental transition as well as Fermi resonances. This has been done in the present case and illustrated in the Results and Discussion section. For the sake of completeness, we mention that more elaborated semiclassical approaches have been developed to decompose each anharmonic semiclassical signal (i.e., wave function) into its harmonic components.[51,52] This procedure would require more work but would also be more directly comparable to MULTIMODE calculations providing better resolved quantum power spectra. However, while MULTIMODE gets all states at once upon diagonalization of an H matrix, SC methods need to focus to one or a few states at a time.

Finally, we note that since AS-SCIVR is a semiclassical method that aims for quantization of the vibrational modes, and notably those corresponding to the OH-stretch and CH-stretch, the expectation is that it will perform well here. Such quantization is absent in MD calculations as well as the TRPMD ones. The MD calculations at best capture some anharmonicity of these modes; however, at 300 K, this is not really achieved given the "stiffness" of these modes. TRPMD

https://doi.org/10.1021/acs.jctc.5c00173
J. Chem. Theory Comput. 2025, 21, 5208−5220

aims to capture anharmonicity visited by zero-point motion, and this is expected and seen to provide a more realistic description of these modes. However, quantization is also absent in TRPMD and so the anharmonicity associated with the vibrationally excited states is not captured by TRPMD. The extent of the missing anharmonicity in both classical and TRPMD calculations and the accuracy of AS-SCIVR is of course problem-specific and an objective here is to quantify this for ethylene glycol. Details of the MD and TPRMD calculations of the power spectra we show here are given in ref 3 and the interested reader is directed there for these details.

RESULTS AND DISCUSSION

PES Fitting. A full-dimensional PES of ethylene glycol has been developed using the PIP approach and this PES has been employed for all results presented in this section. A total of 18,772 geometries have been employed in developing this PES and the data set has been taken from a recently reported article.[3] All electronic energy calculations were performed using the MP2/aug-cc-pVTZ (MP2/aVTZ) level of theory, as described previously.[3] The distribution of these energies is shown in Figure 2. As seen, there is a concentration of energies

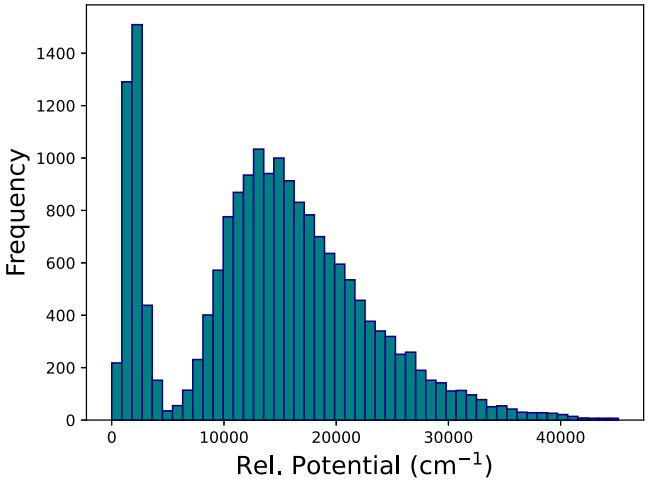

Figure 2. MP2/aug-cc-pVTZ energy distribution of the data set with respect to the minimum energy.

between 0 and roughly 5000 cm^{-1}. These are used to establish a "reaction surface", where the potential is minimized with respect to three dihedral angles, as described in ref 3. Energies for displaced configuration from this minimum surface constitute the second broad distribution of energies. Potential gradients were also reported for these energies and these constitute an additional 563,160 pieces of data.

The PIP basis to fit this PES is generated using MSA software.[15,20] We perform both weighted average and unweighted fitting for this PES. In the process of weighted average fitting, a weight is assigned to each data point based on its energy. The weight is given by wt = $E_0/(E_0 + dE)$, where dE is the energy relative to the minimum in a.u., and E_0 is the parameter that we could modify. For the unweighted fitting, E_0 is typically set as a large number, such as 10^{10} a.u., resulting in all weights essentially being 1. Here we have used E_0 as 0.01 to get the weighted average fitting. The RMSEs for the unweighted and weighted fitting are 124 and 70 cm^{-1} for energies; 0.0009617 hartree/bohr and 0.0005455 hartree/bohr for forces, respectively. We used the weighted average PES for all the studies. A correlation plot between the weighted PES energies and gradients vs corresponding direct MP2 energies and gradients along with the absolute fitting errors for the 18,722 data points is shown in Figure 3.

To examine the standard fidelity of this PES, we first perform geometry optimizations of ten low-lying conformers of ethylene glycol. The structures of nine low-lying conformers of ethylene glycol are shown in Figure 4. A comparison of the relative energetics of these conformers is shown in Table 1. It is seen that PES-optimized conformers perfectly preserved the energy order in accord with the direct MP2/aVTZ energies as well as CCSD(T) ones and also PES-optimized energies are within 30−60 cm^{-1} of the direct MP2/aVTZ energies. Note that although we have shown the relative energies of 10 conformers, the spectrum is thermally well-converged just considering the lowest four energy ones; however, for completeness, we also included the fifth one in the VSCF/VCI calculations.

Next, to examine the vibrational frequency predictions of the PES, we perform normal-mode analyses for five low-lying conformers. The comparison of harmonic mode frequencies for these five conformers with direct MP2/aVTZ ones is shown in Table 2. The agreement with the direct MP2/aVTZ frequencies for these conformers is overall very good; the maximum error is 58 cm^{-1} for the second lowest frequency mode of $\mathbf{g^+Tg^-}$ conformer, but most of the frequencies are within a few cm^{-1} of the ab initio ones, especially the high-frequency OH- and CH-stretches are within 20−25 cm^{-1} of direct MP2 values. And the mean absolute errors (MAEs) are within 12 cm^{-1}. All these local minima are confirmed by obtaining no imaginary frequency except for the $\mathbf{g^-G^+g^-}$ conformer, where we obtained a small imaginary frequency of 67i. This imaginary mode corresponds to the large-amplitude, low-frequency torsional mode. And since this mode, and other low-frequency ones, are not included in the VSCF/VCI calculations (see below) this "issue" is literally of no consequence.

Normal modes 19−22 correspond to the four CH-stretches and 23 and 24 correspond to the two OH-stretches. Of the various bending modes, the highest frequency ones, modes 17 and 18, are of interest as they are roughly in the ratio 1:2 with the CH-stretch modes at 3053 and 3058 cm^{-1}. We return to this in the next section.

MULTIMODE Results. As a quantum nuclear application of the PES, we performed VSCF/VCI calculations using Version 5.1.4 of MULTIMODE.[8,21,23] For all the calculations, a four-mode representation of the potential in mass-scaled normal coordinates and a two-mode representation of the effective inverse moment of inertia for the vibrational angular momentum terms in the exact Watson Hamiltonian are used.[24] The formalism is based on the configuration interaction (CI) approach from the virtual space of the ground vibrational state VSCF Hamiltonian. Here we explore reduced-mode coupling models, i.e., 15-mode models, where these sets of modes start with the highest frequency OH-stretches and proceed in decreasing frequency. In this case, the maximum mode combination excitations are 10 10 10 8, which means that singles through triple excitations extend to a maximum sum of quanta of 10, and for quadruple excitations, the maximum is 8. This excitation space leads to the VCI H-matrix of order 155 026 for the 15-mode calculation. We computed 200 CI vibrational states up to the energy of 4000 cm^{-1}.

https://doi.org/10.1021/acs.jctc.5c00173
J. Chem. Theory Comput. 2025, 21, 5208−5220

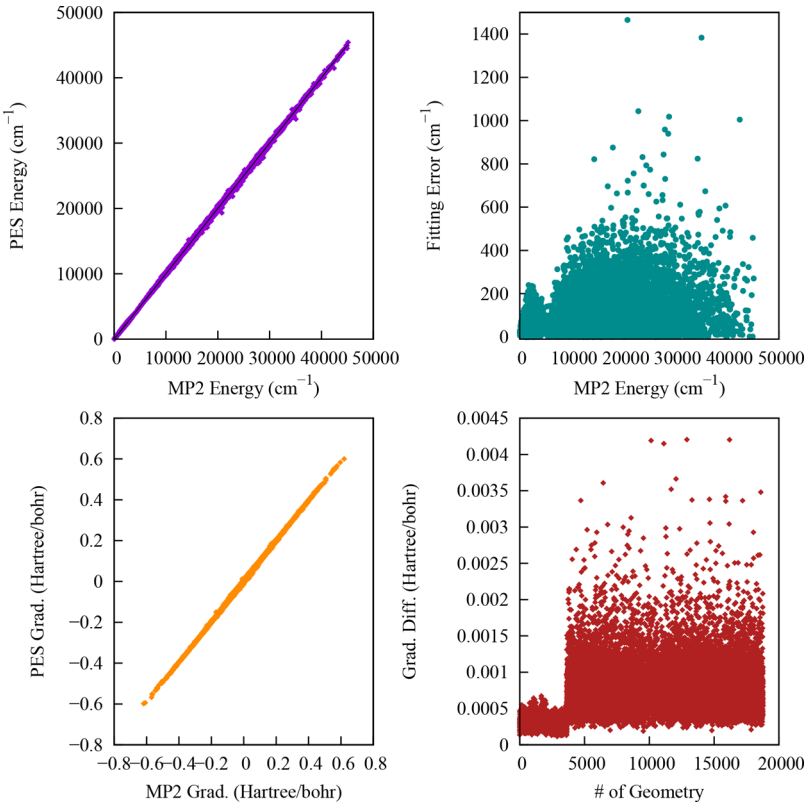

Figure 3. Left upper panel shows the direct MP2 vs PES energies for the training data set relative to the MP2 minimum energy. Corresponding fitting errors relative to the minimum energy are shown in the right upper panels. The left lower panel represents the correlation between the direct MP2 and PES gradients for the training data set. Corresponding gradient fitting errors are shown in the lower right panels.

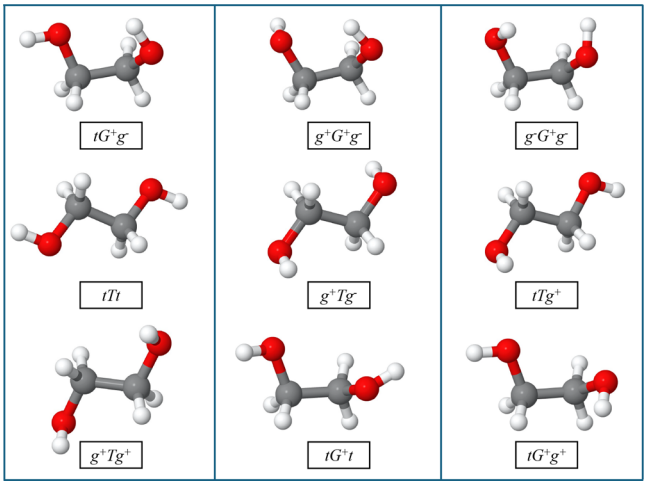

Figure 4. PES optimized geometry of nine low-lying conformers of ethylene glycol.

MULTIMODE calculations were performed for the five low-lying conformers. Table 3 shows MULTIMODE VSCF/VCI frequencies with the corresponding harmonic ones and the three largest VCI coefficients in the expansion basis above for the global minimum conformer ($\mathbf{tG^+g^-}$). Results for other conformers are given in the SI. First, note that the harmonic frequencies are noticeably overestimated compared to the corresponding CI values, particularly for the CH- and OH-stretches, which are overestimated by approximately 200 cm^{-1}. This highlights the impact of anharmonicity, as expected. The presence of mixing states, notably due to Fermi resonances, is also observed. This similar trend we also observed for the other four conformers, and the VCI frequencies with the three largest VCI coefficients are provided in Tables S2−S5 in SI.

The VCI coefficients for states with energies above 1478 cm^{-1} are the ones of interest for the calculation of the power spectrum, according to the remarks above. As seen, the states in the region of the CH-stretch are strongly mixed with overtones and combination bands of the lower-frequency bends. The state at 2798 cm^{-1} is dominantly the combination band $\nu_{15} + \nu_{16}$ with a VCI weight of 0.16 for the CH-stretch.

Table 1. Relative Energetics (cm^{-1}) of Ten Low-Lying Conformers of Ethylene Glycol with Respect to the Global Minimum

method	tG$^+$g$^-$	g$^+$G$^+$g$^-$	g$^-$G$^+$g$^-$	tTt	g$^+$Tg$^-$	tTg$^+$	g$^+$Tg$^+$	tG$^+$t	tG$^+$g$^+$	cCt
MP2/aVTZ[a]	0.0	149	330	912	979	971	1046	1084	1249	2298
CCSD(T)[a]	0.0	113	305	876	908	919	968	1093	1210	2324
PES	0.0	69	290	905	1015	904	972	1115	1219	2252
PES^{wt}	0.0	79	292	912	1018	894	990	1111	1215	2261

[a]From Table S1 in ref 3.

https://doi.org/10.1021/acs.jctc.5c00173
J. Chem. Theory Comput. 2025, 21, 5208−5220

Table 2. Normal Mode Frequencies (cm^{-1}) for Five Low-Lying Conformers of Ethylene Glycol from Weighted Fitting PES

	tG^+g^-		$g^+G^+g^-$		$g^-G^+g^-$		tTt		g^+Tg^-	
mode	MP2/TZ[a]	PES	MP2/TZ[a]	PES	MP2/TZ[a]	PES	MP2/TZ[a]	PES	MP2/TZ[a]	PES
1	168	170	168	167	100	67i	116	132	141	145
2	247	216	292	301	159	167	217	190	250	192
3	329	332	327	326	321	326	230	209	268	223
4	420	407	452	459	428	432	291	295	296	285
5	523	529	536	531	528	530	481	483	475	468
6	887	889	878	874	881	880	839	842	803	787
7	904	905	897	900	885	889	1009	1046	1027	1043
8	1066	1071	1059	1061	1051	1058	1076	1074	1074	1074
9	1100	1098	1073	1073	1063	1073	1094	1090	1090	1083
10	1130	1135	1122	1121	1126	1123	1167	1168	1109	1107
11	1178	1207	1204	1215	1198	1200	1190	1236	1140	1154
12	1269	1277	1246	1250	1257	1280	1235	1241	1320	1337
13	1296	1314	1374	1360	1383	1401	1288	1306	1339	1343
14	1384	1390	1377	1379	1389	1403	1319	1328	1370	1364
15	1420	1429	1406	1405	1404	1414	1409	1427	1404	1381
16	1455	1465	1435	1437	1422	1428	1487	1513	1433	1429
17	1516	1519	1511	1514	1508	1513	1541	1545	1521	1507
18	1524	1525	1521	1519	1512	1526	1551	1549	1535	1535
19	3053	3056	3026	3027	3071	3069	3057	3065	3067	3067
20	3058	3064	3070	3073	3074	3077	3064	3066	3076	3075
21	3114	3118	3134	3136	3140	3142	3102	3104	3124	3127
22	3149	3148	3159	3160	3148	3150	3127	3130	3150	3149
23	3808	3831	3794	3815	3845	3856	3857	3870	3840	3856
24	3856	3871	3831	3847	3846	3876	3858	3878	3842	3869
MAE		**8**		**5**		**8**		**12**		**12**

[a]From Table S3 in ref 3.

Table 3. VSCF/VCI Energies (cm^{-1}) and VCI Expansion Coefficients for the tG^+g^- Conformer

mode	Har. freq	CI freq	VCI coeff.	corresponding modes
10	1135	1119	0.9957	ν_{10}
11	1207	1167	−0.9889, 0.0581, 0.0455	ν_{11}, ν_{12}, ν_{14}
12	1277	1246	0.9774, 0.1745, 0.0632	ν_{12}, ν_{13}, ν_{11}
13	1314	1268	−0.9633, 0.1771, 0.1318	ν_{13}, ν_{12}, ν_{15}
14	1390	1340	0.9344, 0.3043, 0.1418	ν_{14}, ν_{15}, ν_{13}
15	1429	1387	−0.9354, 0.3206, −0.0952	ν_{15}, ν_{14}, ν_{13}
16	1465	1429	−0.9913, −0.0475, 0.0418	ν_{16}, ν_{18}, ν_{15}
17	1519	1472	0.9552, −0.2789, −0.0396	ν_{17}, ν_{18}, ν_{15}
18	1525	1478	0.9549, 0.2799, −0.0395	ν_{18}, ν_{17}, ν_{16}
19	3056	2798	0.8310, −0.3908, 0.2718	$(\nu_{15} + \nu_{16})$, ν_{19}, $2\nu_{16}$
		2918	0.5991, 0.4551, 0.3765	ν_{19}, $2\nu_{18}$, $2\nu_{16}$
		2972	0.6764, −0.3948, 0.3448	ν_{21}, $2\nu_{18}$, ν_{19}
		2981	−0.5441, 0.5289, −0.4209	$(\nu_{17} + \nu_{18})$, ν_{21}, ν_{19}
20	3064	2836	−0.8092, 0.3438, −0.2593	$2\nu_{16}$, $(\nu_{15} + \nu_{15})$, ν_{20}
		2906	−0.8184, 0.2904, −0.2245	$(\nu_{16} + \nu_{17})$, ν_{20}, $(\nu_{17} + \nu_{18})$
		2915	0.5181, 0.4893, 0.4766	$(\nu_{16} + \nu_{17})$, $2\nu_{17}$, ν_{20}
		2961	0.5192, 0.4968, 0.4057	ν_{20}, $(\nu_{17} + \nu_{18})$, $2\nu_{18}$
21	3118	2972	0.6764, −0.3948, 0.3448	ν_{21}, $2\nu_{18}$, ν_{19}
		2981	−0.5441, 0.5289, −0.4209	$(\nu_{17} + \nu_{18})$, ν_{21}, ν_{19}
22	3148	3012	−0.8881, −0.1973, 0.1762	ν_{22}, $2\nu_{17}$, $(\nu_{17} + \nu_{18})$
23	3831	3629	−0.9645, −0.0877, −0.0796	ν_{23}, $(\nu_{11} + 2\nu_{13})$, $(2\nu_{10} + \nu_{15})$
24	3871	3681	0.9600, −0.1649, 0.0869	ν_{24}, $(\nu_{11} + 2\nu_{13})$, ν_{23}

By contrast the states for the OH-stretches, modes 23 and 24 are "pure", i.e., with VCI coefficients of 0.96 in magnitude.

https://doi.org/10.1021/acs.jctc.5c00173
J. Chem. Theory Comput. 2025, 21, 5208−5220

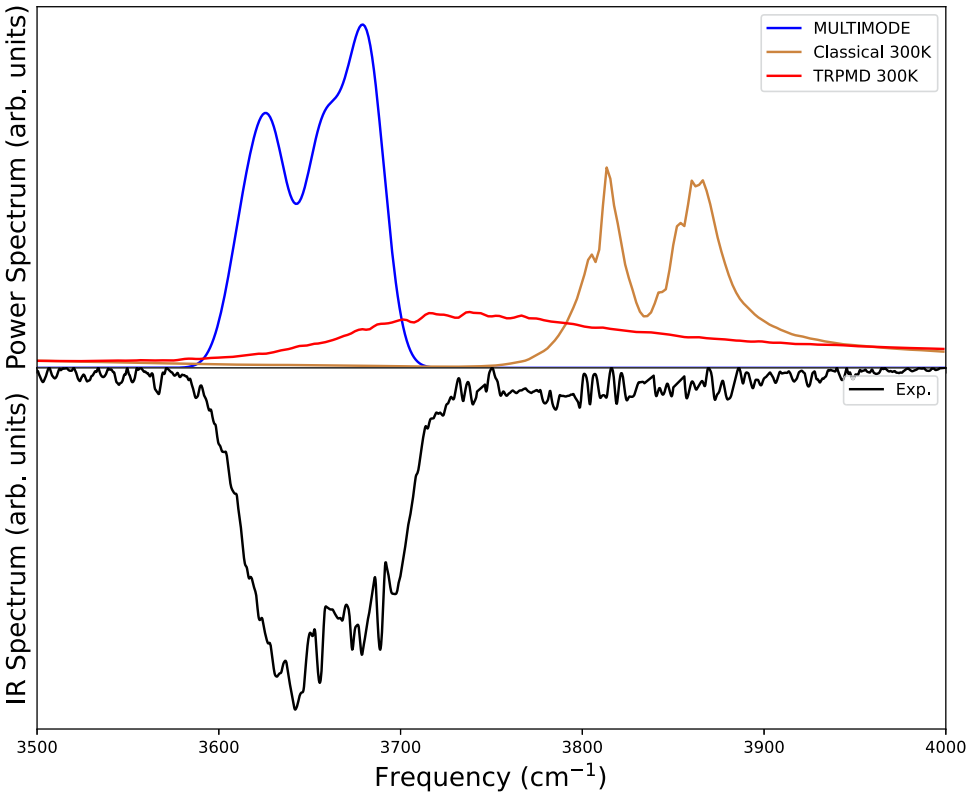

Figure 5. MULTIMODE spectra (blue curve) computed from VSCF/VCI calculations (with Boltzmann-weighted and smoothing by Gaussian broadening), power spectra at 300 K from Classical MD (orange curve) and TRPMD (red curve) simulations from Arandhara et al.[3] compared with experimental IR spectra (black curve) from Das et al.[1] for OH-stretching region. See text for details.

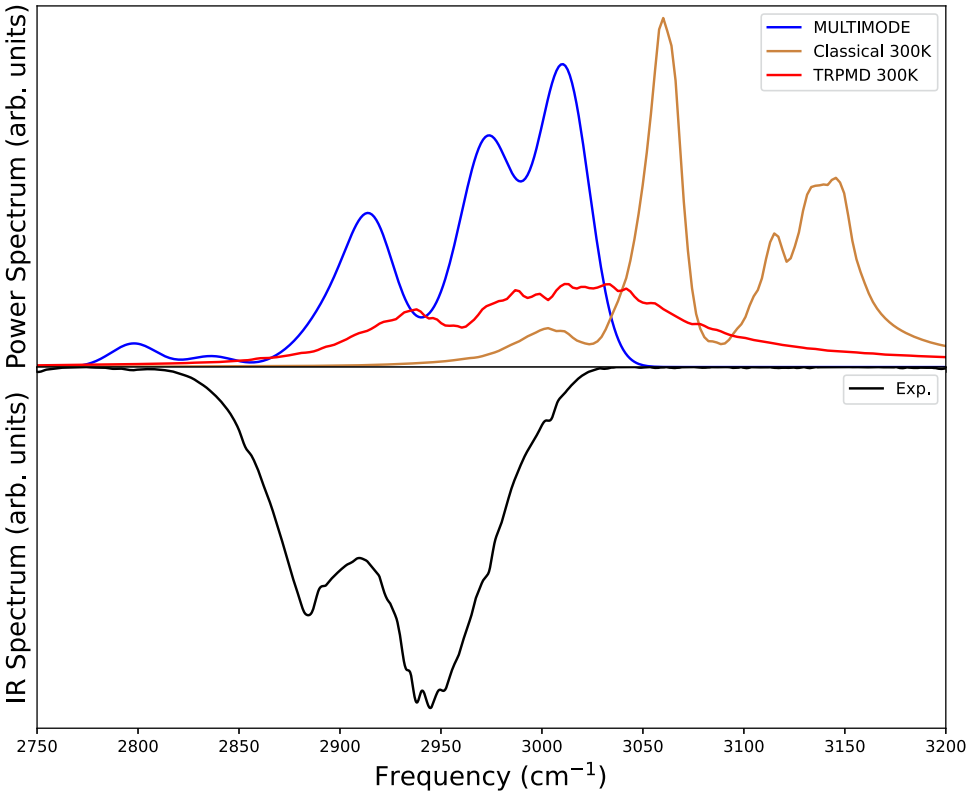

Figure 6. MULTIMODE spectra (blue curve) computed from VSCF/VCI calculations, power spectra at 300 K from classical MD (orange curve), and TRPMD (red curve) simulations from Arandhara et al.[3] compared with experimental IR spectra (black curve) from Das et al.[1] for the CH-stretching region. See text for details, especially for the absence of the MULTIMODE band at 2800 cm^{-1}.

https://doi.org/10.1021/acs.jctc.5c00173
J. Chem. Theory Comput. 2025, 21, 5208−5220

Next, we present the central results of this paper, namely comparisons between theory and experiment for the vibrational spectra of the OH and CH-stretch bands.

OH-Stretch. First, we present the spectra for the OH-stretching modes. We obtained anharmonic OH-stretching frequencies from MULTIMODE calculations as 3629 and 3681 cm^{-1} for the global minimum conformer ($\mathbf{tG^+g^-}$), whereas the harmonic ones are 3831 and 3871 cm^{-1} (From Table 3). Anharmonic OH-stretching frequencies of the other four low-lying conformers are provided in Tables S2−S5 in SI.

The leading expansion coefficients are equal to 0.9 or greater for the OH-stretch VSCF/VCI basis function, as shown in Table 3 and as noted already. Thus, from simple zero-order arguments we expect the power and IR spectra to be quite similar for this fundamental transition. And indeed that is seen. A comparison of anharmonic OH-stretching frequencies with the experimental one and the TRPMD and classical MD power spectra are shown in Figure 5. As we do not have a dipole moment surface of ethylene glycol, obtaining the exact intensities of these corresponding eigenstates is impossible. Therefore, we first try to make a stick plot by taking all anharmonic eigenstates of OH-stretching (obtained from MULTIMODE calculations) for five low-lying conformers and assign an arbitrary intensity of 0.2 for each eigenstate. Then we make thermal averaging of these sticks by multiplying each eigenstate by its corresponding Boltzmann weight. The dotted sticks in Figure S1 in the SI represent the thermally average stick plot of the anharmonic OH-stretching and making it more realistic spectra we apply Gaussian broadening denoted by a blue line.

As seen from Figure 5 (or from Figure S1), the VSCF/VCI power spectrum aligns excellently with the experimental IR spectrum. The classical MD spectrum is in poor agreement with the experiment for this strongly anharmonic band. This is expected, since the peaks in the MD spectrum basically align with the harmonic OH-stretch energies. Finally, while the very broad TRPMD band does exhibit some down-shift anharmonicity, it still overestimates the experimental band peak by about 100 cm^{-1}.

CH-Stretch. Next, we consider the CH-stretch band. As can be surmised from the detailed results shown in Table 3, this band is not as "simple" as the OH-stretch one, owing to large Fermi mixing among the basis states. And, as a result, larger differences between the power and IR spectra are expected, owing to the likely strong variation in IR intensity across the band. We defer a discussion of these resonances and their absence in the TRPMD and classical MD simulations to the Discussion section.

With the above remarks in mind consider the spectral results shown in Figure 6 (the corresponding stick plot of this C−H band is shown in Figure S2 in the SI). As seen, the present VSCF/VCI band is closer to the experimental one than the TRPMD and MD bands, which are upshifted from the experiment by roughly 40 and 80 cm^{-1}, respectively. The VSCF/VCI band at roughly 2800 cm^{-1} is evidently absent in the experimental IR spectrum. This can be explained by examining the results of Table 3 for this band. As seen this lowest energy "CH-stretch" is a strongly mixed state, with the leading VCI coefficient corresponding to the combination band $\nu_{15} + \nu_{16}$ of two bends. Indeed, the sum of the VSCF/VCI energies of these bends equals 2816 cm^{-1} which is quite close to the eigenstate energy of 2798 cm^{-1}. So this band is a combination band, which from elementary considerations is expected to have much smaller IR intensity than a fundamental CH-stretch. Thus, its absence in the experimental IR spectrum is not surprising.

As seen for the OH-stretch, the VSCF/VCI power spectrum aligns much better with the experimental IR spectrum than the classical and TRPMD spectra. The CH-stretch is complex, as noted, owing to multiple resonance interactions with bending modes.

Before presenting the AS-SCIVR results, We note that the TRPMD and classical MD power spectra were obtained using a previous PES by Arandhara and Ramesh,[3] and those in the present calculations using our fit to their data. We verify that MULTIMODE results using the two PESs produce very similar results. This is shown in Table S6 in the SI. Finally, in Table S7 we present VSCF/VCI energies neglecting the vibrational angular momentum terms. As seen, the error due to this is state-dependent, but is about 1 cm^{-1} for many states. This value is, i.e., about a cm^{-1} is consistent with an earlier report of neglecting these terms for H_2O,[23] where the error ranges from several to 10 cm^{-1} for fundamentals.

AS-SCIVR Results. *OH-Stretch.* Starting our description of the semiclassical results from the OH-stretch band, by looking at Figure 7 we notice that AS-SCIVR calculations for the global

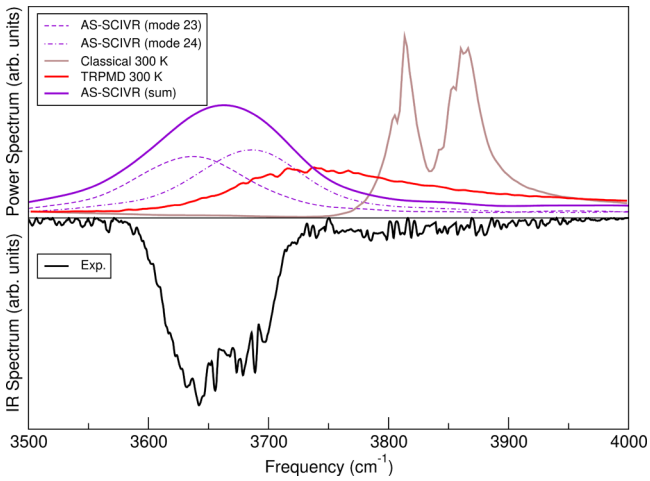

Figure 7. OH-stretch band for the $\mathbf{tG^+g^-}$ conformer. Top panel: AS-SCIVR results for mode 23 (violet, dash), mode 24 (violet, dash, and points), and their sum (violet, solid); TRPMD at 300 K (red); classical (brown). Bottom panel: Experimental results (black).

minimum ($\mathbf{tG^+g^-}$) conformer describe in an excellent way the experimental frequencies, differently from TRPMD and classical simulations which are sizeably shifted to larger frequencies. OH-stretches are estimated by AS-SCIVR at 3685 (mode 24) and 3637 (mode 23) cm^{-1}, which are in excellent agreement with MULTIMODE values of 3681 and 3629 cm^{-1}, respectively.

To present a single curve also for the AS-SCIVR results we sum the two single-mode spectra and scale the outcome in a way that the area below it equals the area below the experimental curve in the 3500−4000 cm^{-1} range. This AS-SCIVR sum-of-states curve is represented with a solid line in Figure 7 with the calculations corresponding to the single modes reported in dashed and dash-and-points lines. The AS-SCIVR sum-of-states curve is a bit wider than the experimental one, but clearly narrower than the TRPMD one. In the case of the AS-SCIVR results, the increased width is due to the fact

https://doi.org/10.1021/acs.jctc.5c00173
J. Chem. Theory Comput. 2025, 21, 5208−5220

that the calculated power spectra include also all states close in frequency to the OH-stretch fundamentals which have a non-negligible projection onto the arbitrary quantum state $|\Psi(q_{eq}, p_{eq})\rangle$ employed in eq 12. Conversely, the IR experimental band is subject to selection rules and dipole strengths which decrease the number of states giving a non-negligible contribution to the band. These factors contribute to reduce the width of the experimental band. We note that the AS-SCIVR method is not "exact" and the broadening of the band was already noted above as being one source of approximation in the AS-SCIVR method.

CH-Stretch. Figure 8 refers to the CH-stretch band and it has been constructed in the same way of Figure 7. AS-SCIVR

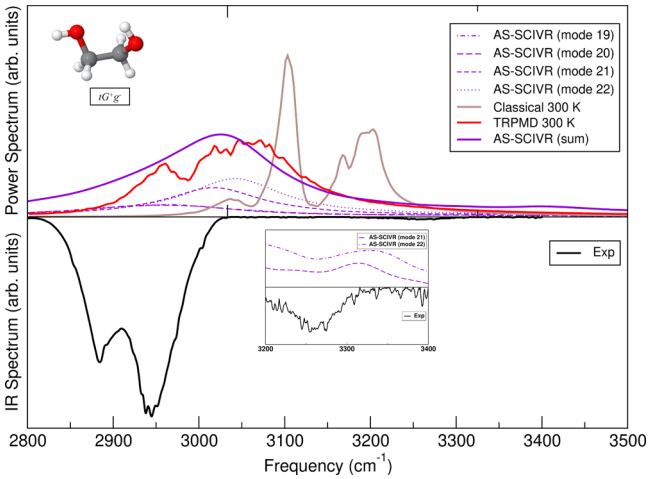

Figure 8. CH-stretch band. Top panel: AS-SCIVR results for modes 19−22 (violet, dashed and points) of the global minimum ($\mathbf{tG^+g^-}$), and their sum (violet, solid); TRPMD calculations at 300 K (red); classical (brown). On bottom panel: experimental results (black); detail of the combination band in the 3200−3300 cm^{-1} region (inset plot).

calculations on the global $\mathbf{tG^+g^-}$ minimum show that there are 4 fundamentals involved in the band. The four single-mode AS-SCIVR spectra can be separated into two groups with peak maxima shifted by about 60 cm^{-1} from the two maxima of the experimental spectrum. The sum-of-states spectrum presents again a single peak slightly more shifted from the experiment than Boltzmann-weighted smoothed MULTIMODE results, but slightly less shifted than TRPMD results. AS-SCIVR estimates the fundamentals of modes 19−22 (the CH-stretch fundamentals) of the global minimum at 2931, 2941, 2989, and 3007 cm^{-1}, respectively. This is on average only 11 cm^{-1} different from MULTIMODE values.

AS-SCIVR results reported in Figure 8 refer to the global minimum conformer only. The necessity to look at other conformers to describe the lower frequency part of the CH-stretch band is confirmed by AS-SCIVR calculations (see below) as it was already pointed out by MULTIMODE ones.

We notice that two fundamental spectral features, which are missed by TRPMD calculations, are remarkably found in the AS-SCIVR simulations. From the insight of Figure 8 it is evident that AS-SCIVR calculations for modes 21 and 22 present a combination band at about 3300 cm^{-1}. This corresponds to the experimental signal of low (but not negligible) intensity just below 3300 cm^{-1}. Remarkably, the shift in the AS-SCIVR estimate of this spectral feature is still 60 cm^{-1} as in the case of the CH-stretch fundamentals. The feature is interpreted as a combination band of these two modes with a low-frequency mode, arguably mode 3. This also explains why the combination is not found in MULTIMODE calculations, since they do not take into account modes with frequency below that of mode 10. Furthermore, no combination band is found in the TRPMD and classical results.

The second feature of AS-SCIVR calculations we want to point out is related to Fermi resonances between the CH stretch and the bending overtone. We find, as shown in Figure S3 of the SI file, that besides the fundamental at 2941 cm^{-1} the AS-SCIVR simulation tailored for mode 19 of the global minimum conformer reports the fingerprint of Fermi resonances by showing two humps at 2884 and 2755 cm^{-1}. Likewise, MULTIMODE anticipates the involvement of mode 19 in Fermi resonances. Conversely, TRPMD is not able to reproduce this feature. Furthermore, the AS-SCIVR simulation detects also for mode 19 a combination band with a low-frequency mode, this time located at 3176 cm^{-1}.

Other Conformers. Finally, we perform AS-SCIVR calculations on two other ethylene glycol conformers, namely the $\mathbf{g^+Tg^-}$ and **tTt** conformers. The goal is to find out if they could be responsible or at least contribute to the lower frequency peak in the experimental CH-stretch band, which is not described by the global minimum $\mathbf{tG^+g^-}$ conformer. Calculations are more difficult because of a higher rejection rate of semiclassical trajectories in part due to the lower coverage of the PES for these two conformers. Thereby, we employ a semiclassical dynamics which is 20,000 a.u. long rather than 25,000 a.u. This allows us to improve the statistics (i.e., convergence) of our calculations at the cost of a lower, but still reasonable, spectral resolution. We find again the presence of Fermi resonances in the CH-stretch bands of these two conformers and, in addition, also stronger coupling between the CH modes. Figures S4 and S5 in the SI file report these calculations. In particular, Figures S4 and S5 (the latter more clearly) demonstrate that AS-SCIVR calculations on these two conformers allow the regain also the lower-frequency part of the CH-stretch band.

For the $\mathbf{g^+Tg^-}$ conformer we find the fundamental frequencies of modes 19−22 at 2929, 2957, 2999, and 3009 cm^{-1}. These values are very close to the MULTIMODE ones presented in Table S5 of the SI file. However, these values appear to be still shifted from the lower peak of the experimental spectrum, which covers a range approximately between 2850 and 2910 cm^{-1}. Moving to the **tTt** conformer, similar coupling features to those found for the previous conformer are present. The four fundamental frequencies are estimated by AS-SCIVR to be at 2864, 2904, 2962, and 3000 cm^{-1}. Therefore, modes 19 and 20 appear to be suitable to describe, at least under the frequency aspect, the lower-frequency end of the experimental CH-stretch band. This is in good agreement with MULTIMODE calculations (see Table S4 in the SI file). Differently from MULTIMODE calculations, though, in the AS-SCIVR calculations mode 19 and mode 20 besides being involved in the usual Fermi resonances appear to be sizably coupled also to mode 21.

SUMMARY AND CONCLUSIONS

We reported a permutationally invariant polynomial fit to 18,772 MP2/aug-cc-pVTZ energies and gradients for ethylene glycol. This potential energy surface was used in VSCF/VCI and semiclassical AS-SCIVR calculations of the power

https://doi.org/10.1021/acs.jctc.5c00173
J. Chem. Theory Comput. 2025, 21, 5208−5220

spectrum in the spectral range of the CH- and OH-stretches for low-lying conformers and compared to experiment and previous TRPMD and classical calculations of the power spectra. The present calculations are in significantly better agreement with the experiment than these previous ones. While the OH-stretch band is dominated by a pure anharmonic OH-stretch, the CH-band is dominated by Fermi resonances with the overtone of bends.

Regarding AS-SCIVR calculations we notice that they have been able to provide VCI-quality results, overperforming classical and TRPMD calculations. AS-SCIVR estimates have accurately described fundamental frequencies of vibrations for both the OH- and CH-stretch bands, as well as Fermi resonances. Furthermore, we remark that AS-SCIVR calculations were performed in full dimensionality, which is fundamental for the description of some spectroscopic features that may be missed by other methods. The latter include combination bands involving low-frequency motions and accurate estimates of the zero-point energy of each conformer. This work confirms the ability of semiclassical methods to accurately reproduce quantum effects when dealing with the spectroscopy (and also kinetics) of sizable molecules and chemical systems[53,54] as in the present case for ethylene glycol or glycine in the past.[55,56] It is also worth mentioning that recent progress in the semiclassical field has permitted to come up with an expression for the calculation of IR spectra,[57] which is analogous to the one employed for power spectra. Therefore, application of the AS-SCIVR technique to IR calculations is anticipated in the near future. The semiclassical techniques employed in this work rely on the pioneering work by Herman and Kluk,[58] and Kaledin and Miller.[59]

Finally, the accuracy of both the VSCF/VCI and AS-SCIVR approaches exceeds that of previous TRPMD and classical MD ones for these bands. The origins of this difference in accuracy is described in detail. This finding is totally consistent with an earlier assessment for protonated water clusters, where, however, only VSCF/VCI, TRPMD, and classical MD were compared.[7]

■ ASSOCIATED CONTENT

Supporting Information

The Supporting Information is available free of charge at https://pubs.acs.org/doi/10.1021/acs.jctc.5c00173.

Details of MULTIMODE input; tables referred to in the text; and figures referred to in the text (PDF)

■ AUTHOR INFORMATION

Corresponding Authors

Apurba Nandi − *Department of Physics and Materials Science, University of Luxembourg, L-1511 Luxembourg City, Luxembourg;* orcid.org/0000-0002-6191-5584; Email: apurba.nandi@uni.lu

Riccardo Conte − *Dipartimento di Chimica, Università degli Studi di Milano, 20133 Milano, Italy;* orcid.org/0000-0003-3026-3875; Email: riccardo.conte1@unimi.it

Joel M. Bowman − *Department of Chemistry and Cherry L. Emerson Center for Scientific Computation, Emory University, Atlanta, Georgia 30322, United States;* orcid.org/0000-0001-9692-2672; Email: jmbowma@emory.edu

Authors

Priyanka Pandey − *Department of Chemistry and Cherry L. Emerson Center for Scientific Computation, Emory University, Atlanta, Georgia 30322, United States;* orcid.org/0000-0002-6930-792X

Paul L. Houston − *Department of Chemistry and Chemical Biology, Cornell University, Ithaca, New York 14853, United States; Department of Chemistry and Biochemistry, Georgia Institute of Technology, Atlanta, Georgia 30332, United States;* orcid.org/0000-0003-2566-9539

Chen Qu − *Independent Researcher, Toronto, Ontario M9B0E3, Canada;* orcid.org/0000-0001-8889-4851

Qi Yu − *Department of Chemistry, Fudan University, Shanghai 200438, P. R. China;* orcid.org/0000-0002-2030-0671

Complete contact information is available at: https://pubs.acs.org/10.1021/acs.jctc.5c00173

Notes

The authors declare no competing financial interest.

■ ACKNOWLEDGMENTS

A.N. thanks Prof. Alexandre Tkatchenko for the financial support from PHANTASTIC grant INTER/MERA22/16521502/PHANTASTIC. J.M.B. thanks NASA, grant 80NSSC22K1167, for financial support. R.C. thanks Università degli Studi di Milano for funding under grant action PSR2023. We thank Prof. Sai G. Ramesh and Mrinal Arandhara for providing us with the training dataset, their PES, and the data to plot the experimental spectrum as well as the classical and TRPMD power spectrum.

■ REFERENCES

(1) Das, P.; Das, P. K.; Arunan, E. Conformational Stability and Intramolecular Hydrogen Bonding in 1,2-Ethanediol and 1,4-Butanediol. *J. Phys. Chem. A* **2015**, *119*, 3710−3720.

(2) Rossi, M.; Ceriotti, M.; Manolopoulos, D. E. How to Remove the Spurious Resonances from Ring Polymer Molecular Dynamics. *J. Chem. Phys.* **2014**, *140*, 234116.

(3) Arandhara, M.; Ramesh, S. G. Nuclear quantum effects in gas-phase ethylene glycol. *Phys. Chem. Chem. Phys.* **2024**, *26*, 19529−19542.

(4) Craig, I. R.; Manolopoulos, D. E. Quantum statistics and classical mechanics: Real time correlation functions from ring polymer molecular dynamics. *J. Chem. Phys.* **2004**, *121*, 3368−3373.

(5) Rossi, M.; Kapil, V.; Ceriotti, M. Fine Tuning Classical and Quantum Molecular Dynamics using a Generalized Langevin Equation. *J. Chem. Phys.* **2018**, *148*, 102301.

(6) Benson, R. L.; Althorpe, S. C. On the "Matsubara heating" of overtone intensities and Fermi splittings. *J. Chem. Phys.* **2021**, *155*, 104107.

(7) Yu, Q.; Bowman, J. M. Classical, Thermostated Ring Polymer, and Quantum VSCF/VCI Calculations of IR Spectra of $H_7O_3^+$ and $H_9O_4^+$ (Eigen) and Comparison with Experiment. *J. Phys. Chem. A* **2019**, *123*, 1399−1409.

(8) Bowman, J. M. Self-consistent Field Energies and Wavefunctions for Coupled Oscillators. *J. Chem. Phys.* **1978**, *68*, 608−610.

(9) Bowman, J. M. The Self-consistent-field Approach to Polyatomic Vibrations. *Acc. Chem. Res.* **1986**, *19*, 202−208.

(10) Christoffel, K.; Bowman, J. Investigations of Self-consistent Field, SCF CI and Virtual state Configuration Interaction Vibrational Energies for a Model Three-mode System. *Chem. Phys. Lett.* **1982**, *85*, 220−224.

(11) Braams, B. J.; Bowman, J. M. Permutationally invariant potential energy surfaces in high dimensionality. *Int. Rev. Phys. Chem.* **2009**, *28*, 577−606.
(12) Qu, C.; Yu, Q.; Bowman, J. M. Permutationally invariant potential energy surfaces. *Annu. Rev. Phys. Chem.* **2018**, *69*, 151−175.
(13) Conte, R.; Parma, L.; Aieta, C.; Rognoni, A.; Ceotto, M. Improved semiclassical dynamics through adiabatic switching trajectory sampling. *J. Chem. Phys.* **2019**, *151*, 214107.
(14) Botti, G.; Aieta, C.; Conte, R. The complex vibrational spectrum of proline explained through the adiabatically switched semiclassical initial value representation. *J. Chem. Phys.* **2022**, *156*, 164303.
(15) *MSA Software with Gradients*, 2019. https://github.com/szquchen/MSA-2.0 (accessed Jan 20, 2019).
(16) Houston, P. L.; Qu, C.; Yu, Q.; Conte, R.; Nandi, A.; Li, J. K.; Bowman, J. M. PESPIP: Software to fit complex molecular and many-body potential energy surfaces with permutationally invariant polynomials. *J. Chem. Phys.* **2023**, *158*, No. 044109.
(17) Bowman, J. M.; Braams, B. J.; Carter, S.; Chen, C.; Czakó, G.; Fu, B.; Huang, X.; Kamarchik, E.; Sharma, A. R.; Shepler, B. C.; Wang, Y.; Xie, Z. Ab-initio-based potential energy surfaces for complex molecules and molecular complexes. *J. Phys. Chem. Lett.* **2010**, *1*, 1866−1874.
(18) Xie, Z.; Bowman, J. M. Permutationally Invariant Polynomial Basis for Molecular Energy Surface Fitting via Monomial Symmetrization. *J. Chem. Theory Comput.* **2010**, *6*, 26−34.
(19) Bowman, J. M.; Czakó, G.; Fu, B. High-dimensional ab initio potential energy surfaces for reaction dynamics calculations. *Phys. Chem. Chem. Phys.* **2011**, *13*, 8094−8111.
(20) Nandi, A.; Qu, C.; Bowman, J. M. Using Gradients in Permutationally Invariant Polynomial Potential Fitting: A Demonstration for CH_4 Using as Few as 100 Configurations. *J. Chem. Theory Comput.* **2019**, *15*, 2826−2835.
(21) Carter, S.; Culik, S. J.; Bowman, J. M. Vibrational Self-consistent Field method for Many-mode Systems: A New Approach and Application to the Vibrations of CO Adsorbed on Cu(100). *J. Chem. Phys.* **1997**, *107*, 10458−10469.
(22) Carter, S.; Bowman, J. M.; Handy, N. C. Extensions and Tests of "Multimode": A Code to Obtain Accurate Vibration/Rotation Energies of Many-Mode Molecules. *Theor. Chem. Acc.* **1998**, *100*, 191−198.
(23) Bowman, J. M.; Carter, S.; Huang, X. MULTIMODE: a Code to Calculate Rovibrational Energies of Polyatomic Molecules. *Int. Rev. Phys. Chem.* **2003**, *22*, 533−549.
(24) Watson, J. K. G. Simplification of the Molecular Vibration-Rotation Hamiltonian. *Mol. Phys.* **1968**, *15*, 479−490.
(25) Ostrowski, L.; Ziegler, B.; Rauhut, G. Tensor Decomposition in Potential Energy Surface Representations. *J. Chem. Phys.* **2016**, *145*, 104103.
(26) Ziegler, B.; Rauhut, G. Efficient Generation of Sum-of-products Representations of High-dimensional Potential Energy Surfaces Based on Multimode Expansions. *J. Chem. Phys.* **2016**, *144*, 114114.
(27) Christiansen, O. Selected New Developments in Vibrational Structure Theory: Potential Construction and Vibrational Wave Function Calculations. *Phys. Chem. Chem. Phys.* **2012**, *14*, 6672−6687.
(28) König, C.; Christiansen, O. Automatic Determination of Important Mode-mode Correlations in Many-mode Vibrational Wave Functions. *J. Chem. Phys.* **2015**, *142*, 144115.
(29) Schröder, B.; Rauhut, G. Incremental Vibrational Configuration Interaction Theory, iVCI: Implementation and Benchmark Calculations. *J. Chem. Phys.* **2021**, *154*, 124114.
(30) Dinu, D. F.; Ziegler, B.; Podewitz, M.; Liedl, K. R.; Loerting, T.; Grothe, H.; Rauhut, G. The Interplay of VSCF/VCI Calculations and Matrix-isolation IR Spectroscopy - Mid Infrared Spectrum of CH_3CH_2F and CD_3CD_2F. *J. Mol. Spectrosc.* **2020**, *367*, No. 111224.
(31) Erfort, S.; Tschöpe, M.; Rauhut, G. Toward a Fully Automated Calculation of Rovibrational Infrared Intensities for Semi-rigid Polyatomic Molecules. *J. Chem. Phys.* **2020**, *152*, 244104.
(32) Schmitz, G.; Artiukhin, D. G.; Christiansen, O. Approximate High Mode Coupling Potentials Using Gaussian Process Regression and Adaptive Density Guided Sampling. *J. Chem. Phys.* **2019**, *150*, 131102.
(33) Madsen, N. K.; Jensen, R. B.; Christiansen, O. Calculating Vibrational Excitation Energies Using Tensor-decomposed Vibrational Coupled-cluster Response Theory. *J. Chem. Phys.* **2021**, *154*, No. 054113.
(34) Moitra, T.; Madsen, D.; Christiansen, O.; Coriani, S. Vibrationally Resolved Coupled-cluster X-ray Absorption Spectra From Vibrational Configuration Interaction Anharmonic Calculations. *J. Chem. Phys.* **2020**, *153*, 234111.
(35) Bowman, J. M.; Carrington, T.; Meyer, H.-D. Variational Quantum Approaches for Computing Vibrational Energies of Polyatomic Molecules. *Mol. Phys.* **2008**, *106*, 2145−2182.
(36) Carter, S.; Bowman, J. M.; Handy, N. C. Multimode calculations of Rovibrational Energies of C_2H_4 and C_2D_4. *Mol. Phys.* **2012**, *110*, 775−781.
(37) Carter, S.; Sharma, A. R.; Bowman, J. M. First-principles Calculations of Rovibrational Energies, Dipole Transition Intensities and Partition Function for Ethylene Using MULTIMODE. *J. Chem. Phys.* **2012**, *137*, 154301.
(38) Roy, T. K.; Gerber, R. B. Vibrational Self-consistent Field Calculations for Spectroscopy of Biological Molecules: New Algorithmic Developments and Applications. *Phys. Chem. Chem. Phys.* **2013**, *15*, 9468−9492.
(39) Oschetzki, D.; Rauhut, G. Pushing the Limits in Accurate Vibrational Structure Calculations: Anharmonic Frequencies of Lithium Fluoride Clusters $(LiF)_n$, n = 2—10. *Phys. Chem. Chem. Phys.* **2014**, *16*, 16426−16435.
(40) Császár, A. G.; Fabri, C.; Szidarovszky, T.; Matyus, E.; Furtenbacher, T.; Czakó, G. The Fourth Age of Quantum Chemistry: Molecules in Motion. *Phys. Chem. Chem. Phys.* **2012**, *14*, 1085−1106.
(41) Tennyson, J. Perspective: Accurate Ro-vibrational Calculations on Small Molecules. *J. Chem. Phys.* **2016**, *145*, 120901.
(42) Wang, X.; Carter, S.; Bowman, J. M. Pruning the Hamiltonian Matrix in MULTIMODE: Test for C_2H_4 and Application to CH_3NO_2 Using a New ab Initio Potential Energy Surface. *J. Phys. Chem. A* **2015**, *119*, 11632−11640.
(43) Carrington, T. Perspective: Computing (Ro-)vibrational Spectra of Molecules with More than Four Atoms. *J. Chem. Phys.* **2017**, *146*, 120902.
(44) Miller, W. H. The semiclassical initial value representation: A potentially practical way for adding quantum effects to classical molecular dynamics simulations. *J. Phys. Chem. A* **2001**, *105*, 2942−2955.
(45) Huber, D.; Heller, E. J. Generalized Gaussian wave packet dynamics. *J. Chem. Phys.* **1987**, *87*, 5302.
(46) Qu, C.; Bowman, J. M. Revisiting Adiabatic Switching for Initial Conditions in Quasi-Classical Trajectory Calculations: Application to CH4. *J. Phys. Chem. A* **2016**, *120*, 4988−4993.
(47) Sun, Q.; Bowman, J. M.; Gazdy, B. Application of adiabatic switching to vibrational energies of three-dimensional HCO, H2O, and H2CO. *J. Chem. Phys.* **1988**, *89*, 3124−3130.
(48) Saini, S.; Zakrzewski, J.; Taylor, H. S. Semiclassical quantization via adiabatic switching. II. Choice of tori and initial conditions for multidimensional systems. *Phys. Rev. A* **1988**, *38*, 3900−3908.
(49) Nagy, T.; Lendvay, G. Adiabatic Switching Extended To Prepare Semiclassically Quantized Rotational-Vibrational Initial States for Quasiclassical Trajectory Calculations. *J. Phys. Chem. Lett.* **2017**, *8*, 4621−4626.
(50) Goldstein, H. *Classical Mechanics*, 2nd ed.; Addison-Wesley: New York, 1988.
(51) Micciarelli, M.; Conte, R.; Suarez, J.; Ceotto, M. Anharmonic vibrational eigenfunctions and infrared spectra from semiclassical molecular dynamics. *J. Chem. Phys.* **2018**, *149*, No. 064115.
(52) Aieta, C.; Micciarelli, M.; Bertaina, G.; Ceotto, M. Anharmonic quantum nuclear densities from full dimensional vibrational

https://doi.org/10.1021/acs.jctc.5c00173
J. Chem. Theory Comput. 2025, 21, 5208−5220

eigenfunctions with application to protonated glycine. *Nat. Commun.* **2020**, *11*, 4348.
(53) Conte, R.; Aieta, C.; Cazzaniga, M.; Ceotto, M. A perspective on the investigation of spectroscopy and kinetics of complex molecular systems with semiclassical approaches. *J. Phys. Chem. Lett.* **2024**, *15*, 7566−7576.
(54) Conte, R.; Mandelli, G.; Botti, G.; Moscato, D.; Lanzi, C.; Cazzaniga, M.; Aieta, C.; Ceotto, M. Semiclassical description of nuclear quantum effects in solvated and condensed phase molecular systems. *Chem. Sci.* **2024**, *16*, 20−28.
(55) Conte, R.; Houston, P. L.; Qu, C.; Li, J.; Bowman, J. M. Full-dimensional, ab initio potential energy surface for glycine with characterization of stationary points and zero-point energy calculations by means of diffusion Monte Carlo and semiclassical dynamics. *J. Chem. Phys.* **2020**, *153*, 244301.
(56) Mandelli, G.; Corneo, L.; Aieta, C. Coupled Cluster Semiclassical Estimates of Experimental Reaction Rates: The Interconversion of Glycine Conformer VIp to Ip. *J. Phys. Chem. Lett.* **2023**, *14*, 9996−10002.
(57) Lanzi, C.; Aieta, C.; Ceotto, M.; Conte, R. A time averaged semiclassical approach to IR spectroscopy. *J. Chem. Phys.* **2024**, *160*, 214107.
(58) Herman, M. F.; Kluk, E. A semiclassical justification for the use of non-spreading wavepackets in dynamics calculations. *Chem. Phys.* **1984**, *91*, 27−34.
(59) Kaledin, A. L.; Miller, W. H. Time averaging the semiclassical initial value representation for the calculation of vibrational energy levels. *J. Chem. Phys.* **2003**, *118*, 7174−7182.

https://doi.org/10.1021/acs.jctc.5c00173
J. Chem. Theory Comput. 2025, 21, 5208−5220